Physica A 517 (2019) 475–483

Contents lists available at ScienceDirect

Physica A

journal homepage: www.elsevier.com/locate/physa

Investigation of the temporal correlations between earthquake magnitudes before the Mexico M8.2 earthquake on 7 September 2017

Nicholas V. Sarlis [a,*], Efthimios S. Skordas [a], Panayiotis A. Varotsos [a], Alejandro Ramírez-Rojas [b], E. Leticia Flores-Márquez [c]

[a] Section of Solid State Physics and Solid Earth Physics Institute, Department of Physics, National and Kapodistrian University of Athens, Panepistimiopolis, Zografos, 157 84, Greece
[b] Departamento de Ciencias Básicas, Universidad Autónoma Metropolitana, Azcapotzalco, México, Mexico
[c] Instituto de Geofisica, Universidad Nacional Autónoma de México, Mexico

HIGHLIGHTS

- DFA reveals precursory changes in the correlations between earthquake magnitudes.
- The origin of the entropy change before the M8.2 earthquake is investigated.
- DFA exponent minimizes just before the minimum of the M8.2 precursory entropy change.

ARTICLE INFO

Article history:
Received 24 June 2018
Received in revised form 6 September 2018
Available online 22 November 2018

Keywords:
Detrended Fluctuation Analysis
Temporal correlations
Natural time of seismicity
Entropy change under time reversal

ABSTRACT

By employing Detrended Fluctuation Analysis (DFA), which has been established as a standard method to investigate long range correlations in nonstationary time series, we study the temporal correlations between the magnitudes of the earthquakes that occurred before the recent deadly Mexico M8.2 earthquake on 7 September 2017 in Chiapas region. Our aim here is to shed light on the origin of the following precursory phenomenon found in our previous publication (Sarlis et al., 2018): Upon considering the analysis of seismicity in the new time domain termed natural time, it was shown that the entropy change of seismicity under time reversal exhibited an important minimum almost 3 months before this major earthquake. Here the application of DFA to earthquake magnitude time series reveals that this minimum of the entropy change of seismicity is preceded as well as followed by characteristic changes of temporal correlations between earthquake magnitudes, which are quantified by the DFA exponent α. In particular, before this minimum the long range correlations breakdown to an almost random behavior possibly turning to anticorrelation ($\alpha \leq 0.5$) while after the minimum (and before the major M8.2 earthquake) long range correlations develop with an exponent α between 0.6 and 0.7.

1. Introduction

Several studies by various authors [1–7] have shown that earthquakes exhibit complex correlations in time, space and magnitude. The observed earthquake scaling laws (e.g., [8]) are widely accepted to indicate the existence of phenomena

* Corresponding author.
E-mail addresses: nsarlis@phys.uoa.gr (N.V. Sarlis), eskordas@phys.uoa.gr (E.S. Skordas), pvaro@otenet.gr (P.A. Varotsos), arr@correo.azc.uam.mx (A. Ramírez-Rojas), leticia@geofisica.unam.mx (E.L. Flores-Márquez).

https://doi.org/10.1016/j.physa.2018.11.041
0378-4371/

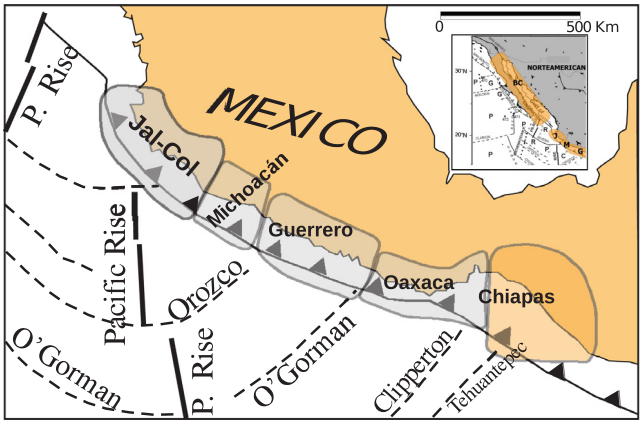

Fig. 1. (Color online) Map of Mexico showing 5 (out of 6) tectonic regions studied in natural time by Ramírez-Rojas and Flores-Márquez [17]: Chiapas (CH), Oaxaca (O), Guerrero (G), Michoacan (M) and Jalisco–Colima (J). A sixth tectonic region, i.e., Baja California (BC) was also studied in Ref. [17] which is shown in the inset.

closely associated with the proximity of the system to a critical point, e.g., [9]. Taking this view that earthquakes are critical phenomena (where a mainshock is the new phase), the quantity by which one can identify the approach of a dynamical system to the state of criticality is termed order parameter. This parameter can be defined in the frame of a new time domain termed natural time and for the case of seismicity is [10] the quantity κ_1 (which stands for the variance of natural time), as explained in detail in Ref. [10] as well as in pp. 249–254 of Ref. [11]. Remarkably, on the basis of this new view of time, a new method of the estimation of seismic risk, termed nowcasting approach [12–15], has been developed.

In a previous paper [16], upon analyzing the seismicity in natural time during the 6-year period 2012–2017 we showed that the occurrence of the M8.2 earthquake on 7 September 2017, which is Mexico's largest earthquake in more than a century, should not be considered unexpected. This earthquake occurred in the Chiapas region (CH) where the probability for the occurrence of an extreme event was found by natural time analysis to be the highest compared to five other tectonic regions, i.e., Baja California (BC), Jalisco–Colima (J), Michoacán(M), Guerrero (G) and Oaxaca (O) of the Mexican Pacific Coast (Fig. 1) in which the seismicity has been studied in natural time by Ramírez-Rojas and Flores-Márquez in Ref. [17] (the selection of these areas is based on tectonic and geological grounds discussed in Ref. [17]).

Furthermore, in Chiapas region, the same analysis revealed that the entropy change ΔS under time reversal exhibited a pronounced minimum on 14 June 2017, i.e., almost 3 months before the occurrence of this M8.2 earthquake. This reflects that an extreme event was likely to take place in this region in view of the following point: When considering the Olami–Feder–Christensen (OFC) model for earthquakes [18], which is probably [19] the most studied non-conservative, supposedly, self-organized criticality (SOC) model (see also [20]), we found that the value of the entropy change under time reversal shows a clear minimum [11] before a large avalanche which corresponds to a large earthquake. Subsequently, we showed [21] that this precursory ΔS minimum on 14 June 2017 is accompanied also by precursory changes of the complexity measure Λ defined [11,22] in natural time associated with the fluctuations of the entropy change under time reversal. In particular, this complexity measure exhibited an abrupt increase approximately on 14 June 2017. Such a behavior of this complexity measure has been found to appear when a complex system approaches the critical point (dynamic phase transition) as, for example, is the case of an impending sudden cardiac death risk [23,24], see section 9.4 of Ref. [11].

It is the scope of this paper to shed more light on the origin of the aforementioned precursory phenomenon that appeared on 14 June 2017. In particular, we shall investigate whether this precursory phenomenon is associated with changes of temporal correlations between earthquake magnitudes. This investigation is made here by employing Detrended Fluctuation Analysis (DFA) which has been established as a standard method to study long range correlations in nonstationary time series. The background of this method is shortly summarized in the next Section and the data analyzed are presented in Section 3 along with a short description of the analysis. The results of the application of DFA to the earthquake magnitude time series of the events that preceded the major M8.2 earthquake are presented in Section 4. Finally, our conclusions are summarized in Section 5.

2. Detrended fluctuation analysis. Background

DFA [25–33] is a method that has been developed, as mentioned, to address the problem of accurately quantifying long range correlations in non-stationary fluctuating signals. It has been applied to a multitude of cases including DNA [34], human motor activity [35] and gait [36], cardiac dynamics [37–39], meteorology [40], climate temperature fluctuations [41], solar incident flux [42]. Traditional methods such as power spectrum and autocorrelation analysis [43] are not suitable for non-stationary signals [29,33].

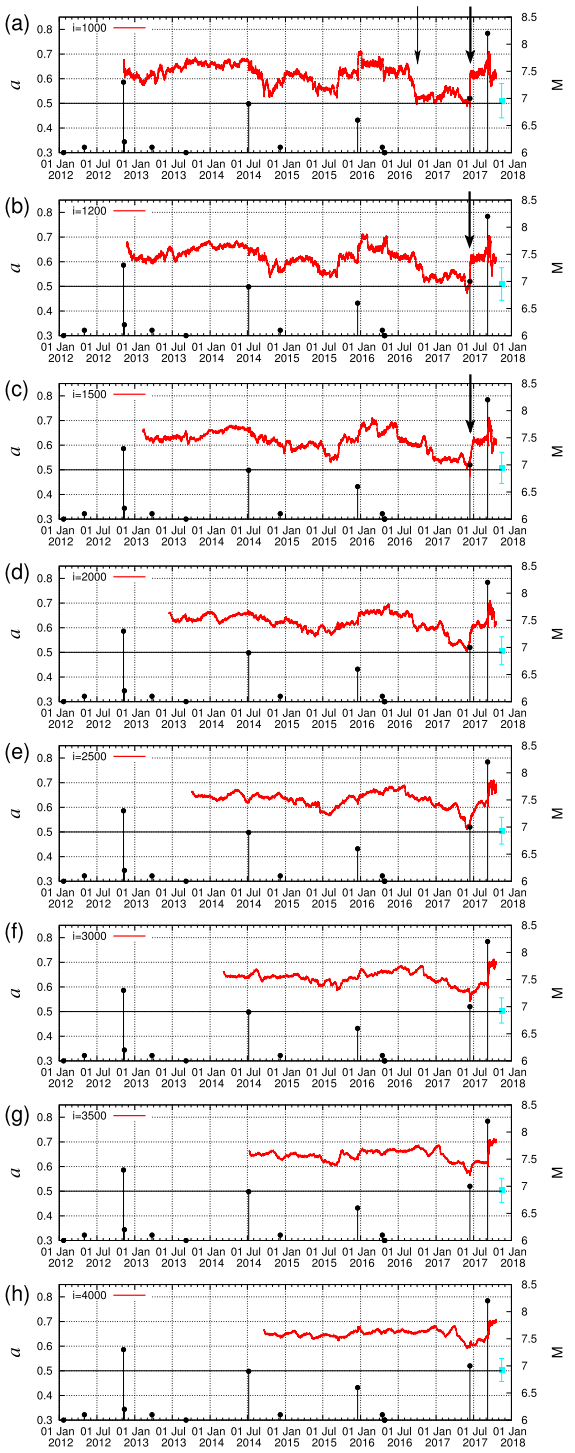

Fig. 2. (Color online) Plot of the a exponent of DFA versus the conventional time. Panels a, b, c, d, e, f, g, and h correspond to the sizes $i = 1000, 1200, 1500, 2000, 2500, 3000, 3500$ and 4000 events, respectively, when analyzing all earthquakes with $M \geq 3.5$. The vertical lines ending at circles depict the earthquake magnitudes which are read in the right scale. The arrows indicate the dates at which a becomes smaller than 0.5 in the shorter sizes. The cyan square with error bars depicts the mean value and the 95% confidence interval for the statistics of the exponent a obtained after randomly shuffling the original magnitude time-series 10^2 times.

DFA consists of the following steps: Starting with a signal $u(k)$, where $k = 1, 2, \ldots, N$, and N is the length of the signal, the first step is to integrate $u(k)$ and obtain

$$y(k) = \sum_{j=1}^{k} [u(j) - \bar{u}] \tag{1}$$

where $\bar{u}$ stands for the mean

$$\bar{u} = \frac{1}{N} \sum_{j=1}^{N} u(j). \tag{2}$$

We then divide the profile $y(k)$ into boxes of equal length n. In each box, we fit $y(k)$ using a polynomial function $y_n(k)$ which represents the local trend in that box. Next, the profile $y(k)$ is detrended by subtracting the local trend $y_i(k)$ in each box of length n:

$$Y_n(k) = y(k) - y_n(k). \tag{3}$$

Finally, the rms fluctuation for the integrated and detrended signal is calculated

$$F(n) \equiv \sqrt{\frac{1}{N} \sum_{k=1}^{N} [Y_n(k)]^2}. \tag{4}$$

The behavior of $F(n)$ over a broad number of scales is obtained by repeating the aforementioned calculation of $F(n)$ for varied box length n. For scale invariant signals, we find:

$$F(n) \propto n^{\alpha} \tag{5}$$

where α is the scaling exponent. If $\alpha = 0.5$, the signal is uncorrelated (white noise), while if $\alpha > 0.5$ the signal is correlated [29–33], i.e., exhibits long range correlations, while if $\alpha < 0.5$ anticorrelated behavior occurs.

By employing DFA it was found [44–46] that long–Range correlations exist (with a signature of criticality) in the so called seismic electric signals (SES) activities which are series of low frequency ($\leq$1 Hz) electric signals that precede earthquakes [47–50] by a lead time ranging from a few weeks to 5.5 months [11]. These signals are emitted from the preparation focal area of an earthquake [51] when the gradually increasing stress before the earthquake occurrence reaches a critical value in which the electric dipoles formed due to point defects [52,53] exhibit cooperative orientation, thus a transient electric signal emerges. DFA has been also employed for the study of seismic time series in various regions, e.g. see Ref. [5] for the Italian territory. DFA studies of the long-term seismicity in Northern and Southern California were initially focused on the regimes of stationary seismic activity and found that long range correlations exist [3,4] between earthquake magnitudes with $\alpha = 0.6$. Similar DFA studies of long-term seismicity were later [54,55] extended also to the seismic data of Japan. In addition, nonextensive statistical mechanics pioneered by Tsallis [56,57] has been employed [55] in order to investigate whether it can reproduce the observed seismic data fluctuations. In this framework, a generalization of the Gutenberg–Richter (G–R) law for seismicity has been offered (for details and relevant references see Section 6.5 of Ref. [11] as well as Ref. [7]) and the investigation led to the following conclusions [11,55]: The results of the natural time analysis of synthetic seismic data obtained from either the conventional G–R law or its nonextensive generalization, deviate markedly from those of the real seismic data. On the other hand, if temporal correlations between earthquake magnitudes identified by DFA, will be inserted to these synthetic seismic data, the results of natural time analysis agree well with those obtained from the real seismic data.

Furthermore, by applying DFA to the earthquake magnitude time series in Japan it was found [58] that the minimum of the fluctuations of the order parameter of seismicity observed before a M $\geq$ 7.8 earthquake appears when long range correlations prevail ($\alpha > 0.5$). Such a minimum emerges simultaneously with the initiation of an SES activity [59]. This minimum is also preceded by a stage in which DFA reveals a clear anti-correlated behavior ($\alpha < 0.5$) between earthquake magnitudes as well as followed by another stage in which long range correlations breakdown to an almost random behavior turning to anticorrelation ($\alpha \leq 0.5$) [58]. Note that such minima of the fluctuations of the order parameter of seismicity have been observed [60,61] before all shallow earthquakes with M $\geq$ 7.6 in Japan during the 27 year period from 1 January 1984 to 11 March 2011, the date of Tohoku earthquake occurrence.

3. Data and analysis

The seismic data we analyzed refer to the Chiapas region, discussed in the second paragraph of the Introduction, (i.e., where the M8.2 earthquake occurred) covering an almost six year period, i.e., from 1 January 2012 until 20 October 2017, and come from the seismic catalog of the National Seismic Service (SSN) of the Universidad Nacional Autónoma de México (www.ssn.unam.mx) To assure catalog completeness a magnitude threshold, i.e., M $\geq$ 3.5 , has been imposed. In addition, a magnitude threshold M $\geq$ 4.0 has been also employed in order to assure that the results obtained are not affected by the value of the magnitude threshold chosen.

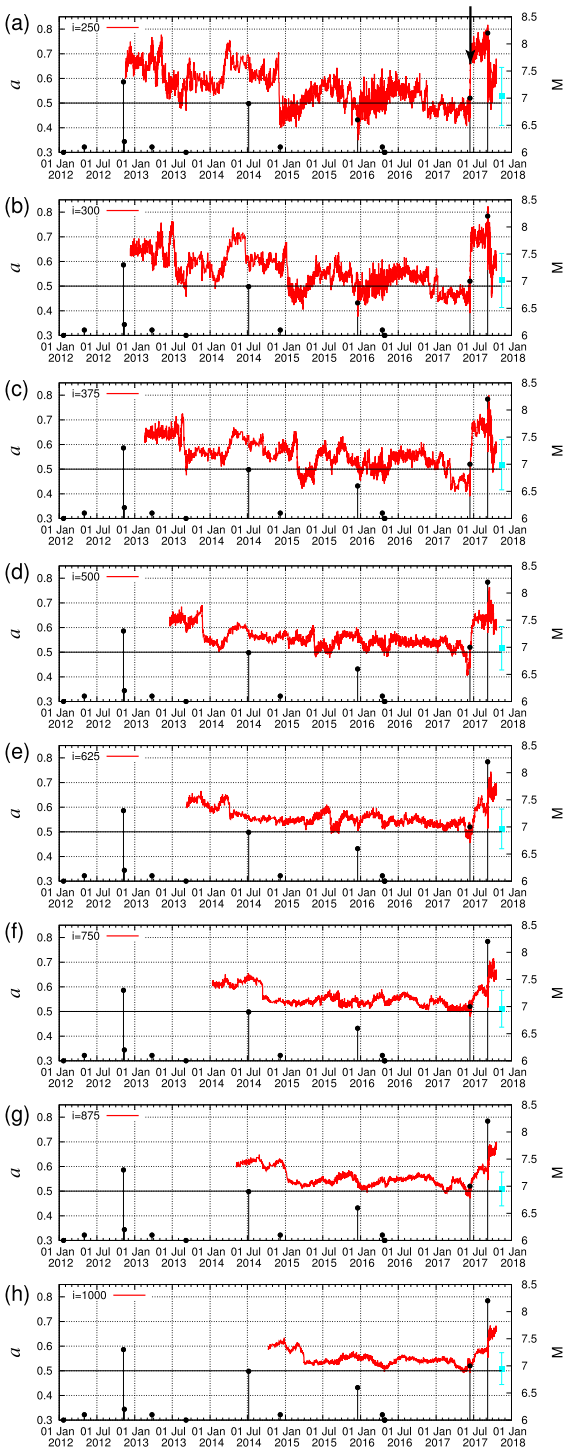

Fig. 3. (Color online) Plot of the a exponent of DFA versus the conventional time. Panels a, b, c, d, e, f, g, and h correspond to the sizes $i = 250, 300, 375, 500, 625, 750, 875$ and 1000 events, respectively, when analyzing all earthquakes with $M \geq 4.0$. The vertical lines ending at circles depict the earthquake magnitudes which are read in the right scale. The arrow in panel (a) indicates the date at which a becomes smaller than 0.5 at all sizes. The cyan square with error bars depicts the mean value and the 95% confidence interval for the statistics of the exponent a obtained after randomly shuffling the original magnitude time-series 10^2 times.

Concerning the calculation procedure, a window of length i (= number of successive events) is sliding, each time by one event, through the whole time series comprising of L events in total and the corresponding earthquake magnitudes,

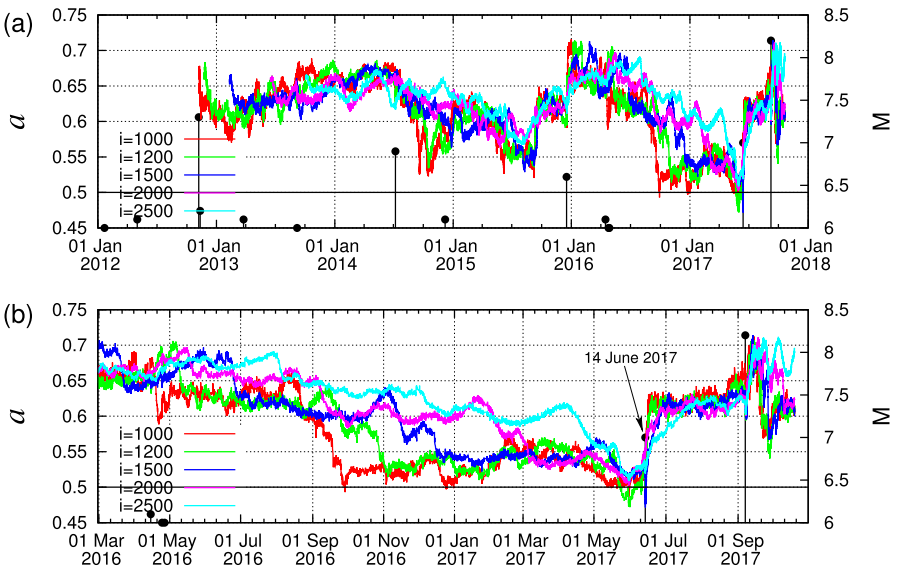

Fig. 4. (Color online) Compilation of plots at the shorter sizes i of the a exponent of DFA versus the conventional time during the six year period (a) 2012–2017 and (b) the one and a half year period from 1 March 2016 until 20 October 2017, when analyzing all earthquakes with $M \geq 3.5$. The vertical lines ending at circles depict the earthquake magnitudes which are read in the right scale.

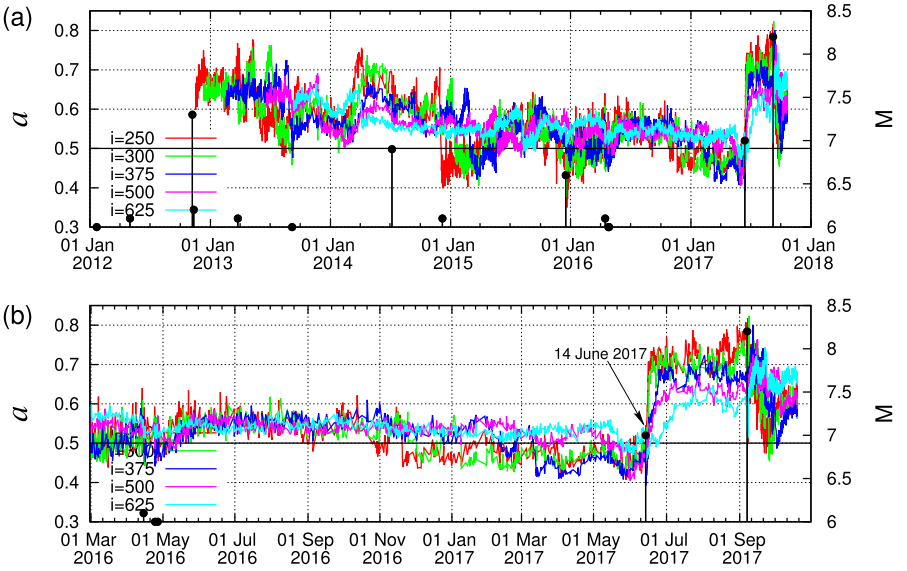

Fig. 5. (Color online) Compilation of plots at the shorter sizes i of the a exponent of DFA versus the conventional time during the six year period (a) 2012–2017 and (b) the one and a half year period from 1 March 2016 until 20 October 2017, when analyzing all earthquakes with $M \geq 4.0$. The vertical lines ending at circles depict the earthquake magnitudes which are read in the right scale.

e.g., $\{M_{j+n}, n = 1, 2, \ldots, i\}$ for the jth window starting from the $j+1$ event of the catalog, $j = 0, 1, \ldots, L-i$, have been analyzed by DFA as described in the preceding Section for $N = i$. The corresponding exponent α of the DFA is attributed to the next M_{j+i+1} 'target' earthquake (cf. when we are interested on the prediction of a target earthquake, we are focusing only on its previous events). As for the values of the window lengths i chosen, they are more or less comparable with those used in Ref. [16] and their selection could be summarized as follows: Since $L \sim 11,500$ earthquakes ($M \geq 3.5$) occurred in the Chiapas region from 1 January 2012 until the occurrence of the M8.2 earthquake on 7 September 2017, we find an average of around 170 earthquakes per month. (This number of earthquakes becomes smaller by a factor of 4 if we adopt, instead of $M \geq 3.5$, the magnitude threshold $M \geq 4.0$.) The smallest length of the time window, hereafter simply called size, employed is $i \sim 10^3$ events (for $M \geq 3.5$) since it corresponds to the number of events that occurs in a time period around the maximum lead time of SES activities which, as mentioned, is 5.5 months. The value of the smallest size becomes

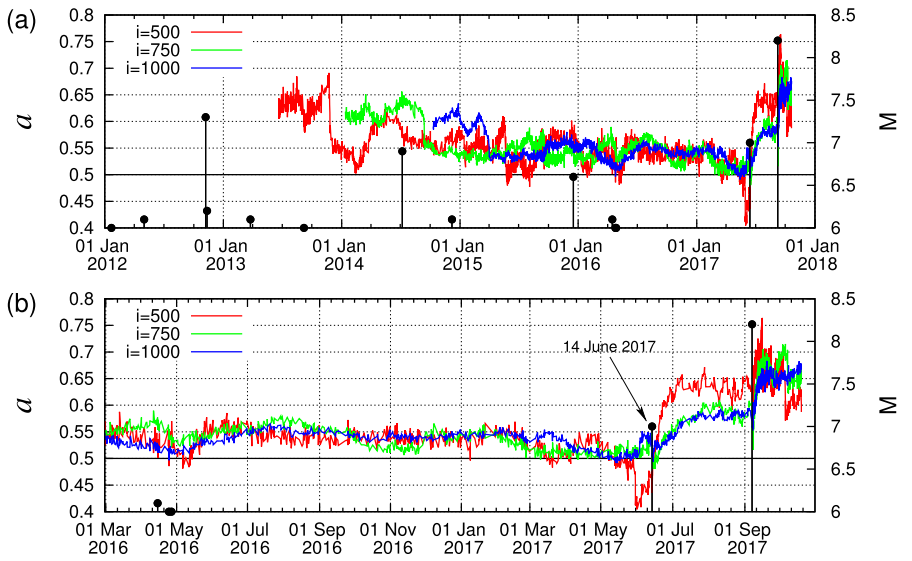

Fig. 6. Plot of the a exponent of DFA versus the conventional time when analyzing all earthquakes with $M \geq 4.0$ and comparing one shorter size (i.e., $i = 500$ events, red) with two of the longer sizes (i.e., $i = 750$ and $i = 1000$ events, green and blue, respectively). The results are shown during the six year period (a) 2012–2017 and (b) the one and a half year period from 1 March 2016 until 20 October 2017. The vertical lines ending at circles depict the earthquake magnitudes which are read in the right scale.

smaller, i.e., $i = 250$, if we alternatively consider the magnitude threshold M $\geq$ 4.0. As for the longest size (for M $\geq$ 3.5) we employ the value $i = 4000$ events since it corresponds to the average number of events that occur in around 2 year period and in addition there is a widespread belief that the earthquake preparation process may start years before the occurrence of large earthquakes of magnitude 8 or larger (e.g., see Ref. [62]).

4. Results and discussion

Fig. 2 a, b, c, d, e, f, g and h depict, for M $\geq$ 3.5 the values of the exponent α of DFA versus the conventional time for the sizes $i = 1000$, 1200, 1500, 2000, 2500, 3000, 3500 and 4000 events, respectively.

A first inspection of the eight sizes depicted in this figure shows that the value of the exponent α becomes smaller than 0.5 in a few dates (these cases are marked with the two arrows in Fig. 2a) only in the shorter sizes, i.e., $i = 1000$, 1200 and 1500 events (M $\geq$ 3.5). For the sake of comparison, we now present in Fig. 3 the results obtained when the magnitude threshold is M $\geq$ 4.0 in a similar fashion as we plotted the corresponding results when we considered M $\geq$ 3.5 in Fig. 2. In particular, in Fig. 3 we plot these α values versus the conventional time. A close inspection of Fig. 3 reveals that at all sizes only at the date marked with a thick arrow the value of the α exponent becomes smaller than 0.5 (i.e., anticorrelated behavior) almost simultaneously with the thicker arrow in Fig. 2. To better visualize this phenomenon the six year results of Figs. 2 and 3 are compiled in Figs. 4a and 5a, respectively. In order to have an appreciably better view, excerpts of Figs. 4a and 5a are shown in Figs. 4b and 5b, respectively, in an expanded scale for the five shorter sizes out of the eight. They present the results only during the period after 1 March 2016, i.e., only almost one and a half year before the M8.2 earthquake. A close inspection of Fig. 4b reveals that at least during the first few months the α values lie between 0.65 and 0.7, but afterwards they gradually diminish. In other words, the α values start to gradually diminish around one year before the M8.2 earthquake occurrence. Quite interestingly, the minima of these α values lying very close to $\alpha \approx 0.5$ (except of the size $i = 1200$ events which shows $\alpha < 0.5$) occur just before 14 June 2017, which is approximately the date of the pronounced entropy change under time-reversal reported in Ref. [16]. Similar conclusions can be drawn more or less from an inspection of Fig. 5b except of the following point: The minimum of the α values in Fig. 5b seems to become lower than 0.5, thus the behavior before the ΔS minimum seems to be anticorrelated. This can be better visualized in Fig. 6 where for $M \geq 4.0$ we compile one of the shorter sizes, i.e., $i = 500$ events, with two of the longer sizes, i.e., 750 and 1000 events. Obviously, before 14 June 2017 the results for the shorter size (red) show $\alpha < 0.5$, i.e., anti-correlation, while the results for the longer sizes (green and blue, respectively) lead to α values close to 0.5. Furthermore, we note that both Figs. 4b and 5b (as well as Fig. 6) clearly show that just after 14 June 2017 the α values increase lying between 0.6 and 0.7 thus long-range temporal correlations develop.

5. Summary and conclusions

In our previous publication [16] by employing natural time analysis of seismicity in the Chiapas region we found that the entropy change ΔS of the seismicity under time reversal exhibited a clear minimum on 14 June 2017. This signaled that a

major event was going to occur in this region, as actually happened almost three months later upon the occurrence of the M8.2 earthquake on 7 September 2017.

Here, we shed light on the origin of this minimum by demonstrating that it is accompanied by the appearance of characteristic changes of temporal correlations between earthquake magnitudes. In particular, upon applying DFA to the earthquake magnitude time series by using sliding natural time windows comprising a number of seismic events that occur within periods of the order of several months, we find that the value of the corresponding DFA exponent α exhibits the following changes: Before the ΔS minimum on 14 June 2017, the exponent α starts to exhibit a gradual decrease from $\alpha \approx 0.6$ down to around $\alpha \leq 0.5$, thus the long-range temporal correlations between earthquake magnitudes breakdown to an almost random behavior possibly turning to anticorrelation. After the ΔS minimum and before the M8.2 earthquake occurrence on 7 September 2017, the exponent α increases to values between 0.6 and 0.7, thus showing that long-range temporal correlations between earthquake magnitudes develop. This is consistent with an earlier finding [58,59] that when an SES activity appears, with a lead time from a few weeks to 5.5 months before a major earthquake, long-range temporal correlations develop between earthquake magnitudes.

References

[1] Q. Huang, Seismicity changes prior to the Ms8.0 Wenchuan earthquake in Sichuan, China, Geophys. Res. Lett. 35 (2008) L23308, http://dx.doi.org/10.1029/2008GL036270.

[2] Q. Huang, Retrospective investigation of geophysical data possibly associated with the Ms8.0 Wenchuan earthquake in Sichuan, China, J. Asian Earth Sci. 41 (2011) 421–427, http://dx.doi.org/10.1016/j.jseaes.2010.05.014.

[3] S. Lennartz, V.N. Livina, A. Bunde, S. Havlin, Long-term memory in earthquakes and the distribution of interoccurrence times, Europhys. Lett. 81 (2008) 69001, http://dx.doi.org/10.1209/0295-5075/81/69001.

[4] S. Lennartz, A. Bunde, D.L. Turcotte, Modelling seismic catalogues by cascade models: Do we need long-term magnitude correlations? Geophys. J. Int. 184 (2011) 1214–1222, http://dx.doi.org/10.1111/j.1365-246X.2010.04902.x.

[5] L. Telesca, V. Lapenna, M. Macchiato, Spatial variability of the time-correlated behaviour in italian seismicity, Earth Planet. Sci. Lett. 212 (2003) 279–290, http://dx.doi.org/10.1016/S0012-821X(03)00286-3.

[6] L. Telesca, M. Lovallo, Non-uniform scaling features in central Italy seismicity: A non-linear approach in investigating seismic patterns and detection of possible earthquake precursors, Geophys. Res. Lett. 36 (2009) L01308, http://dx.doi.org/10.1029/2008GL036247.

[7] L. Telesca, Maximum Likelihood Estimation of the Nonextensive Parameters of the Earthquake Cumulative Magnitude Distribution, Bull. Seismol. Soc. Am. 102 (2012) 886–891, http://dx.doi.org/10.1785/0120110093.

[8] D.L. Turcotte, Fractals and Chaos in Geology and Geophysics, second ed., Cambridge University Press, Cambridge, 1997.

[9] J.R. Holliday, J.B. Rundle, D.L. Turcotte, W. Klein, K.F. Tiampo, A. Donnellan, Space–time clustering and correlations of major earthquakes, Phys. Rev. Lett. 97 (2006) 238501, http://dx.doi.org/10.1103/PhysRevLett.97.238501.

[10] P.A. Varotsos, N.V. Sarlis, H.K. Tanaka, E.S. Skordas, Similarity of fluctuations in correlated systems: The case of seismicity, Phys. Rev. E 72 (2005) 041103, http://dx.doi.org/10.1103/physreve.72.041103.

[11] P.A. Varotsos, N.V. Sarlis, E.S. Skordas, Natural Time Analysis: The new view of time, in: Precursory Seismic Electric Signals, Earthquakes and other Complex Time-Series, Springer-Verlag, Berlin Heidelberg, 2011, http://dx.doi.org/10.1007/978-3-642-16449-1.

[12] J.B. Rundle, D.L. Turcotte, A. Donnellan, L. Grant Ludwig, M. Luginbuhl, G. Gong, Nowcasting earthquakes, Earth Space Sci. 3 (2016) 480–486, http://dx.doi.org/10.1002/2016EA000185.

[13] J.B. Rundle, M. Luginbuhl, A. Giguere, D.L. Turcotte, Natural time, nowcasting and the physics of earthquakes: Estimation of seismic risk to global megacities, Pure Appl. Geophys. 175 (2) (2018) 647–660, http://dx.doi.org/10.1007/s00024-017-1720-x.

[14] M. Luginbuhl, J.B. Rundle, A. Hawkins, D.L. Turcotte, Nowcasting earthquakes: A comparison of induced earthquakes in oklahoma and at the geysers, california, Pure Appl. Geophys. 175 (1) (2018) 49–65, http://dx.doi.org/10.1007/s00024-017-1678-8.

[15] M. Luginbuhl, J.B. Rundle, D.L. Turcotte, Natural time and nowcasting earthquakes: Are large global earthquakes temporally clustered? Pure Appl. Geophys. 175 (2) (2018) 661–670, http://dx.doi.org/10.1007/s00024-018-1778-0.

[16] N.V. Sarlis, E.S. Skordas, P.A. Varotsos, A. Ramírez-Rojas, E.L. Flores-Márquez, Natural time analysis: On the deadly Mexico M8.2 earthquake on 7 September 2017, Physica A 506 (2018) 625–634, http://dx.doi.org/10.1016/j.physa.2018.04.098.

[17] A. Ramírez-Rojas, E.L. Flores-Márquez, Order parameter analysis of seismicity of the Mexican Pacific coast, Physica A 392 (2013) 2507–2512, http://dx.doi.org/10.1016/j.physa.2013.01.034.

[18] Z. Olami, H.J.S. Feder, K. Christensen, Self-organized criticality in a continuous, nonconservative cellular automaton modeling earthquakes, Phys. Rev. Lett. 68 (1992) 1244–1247, http://dx.doi.org/10.1103/physrevlett.68.1244.

[19] O. Ramos, E. Altshuler, K.J. Måløy, Quasiperiodic events in an earthquake model, Phys. Rev. Lett. 96 (2006) 098501, http://dx.doi.org/10.1103/physrevlett.96.098501.

[20] F. Caruso, H. Kantz, Prediction of extreme events in the OFC model on a small world network, Eur. Phys. J. B 79 (2011) 7–11, http://dx.doi.org/10.1140/epjb/e2010-10635-5.

[21] A. Ramírez-Rojas, E.L. Flores-Márquez, N.V. Sarlis, P.A. Varotsos, The complexity measures associated with the fluctuations of the entropy in natural time before the deadly mexico m8.2 earthquake on 7 september 2017, Entropy 20 (6) (2018) 477, http://dx.doi.org/10.3390/e20060477.

[22] N.V. Sarlis, S.-R.G. Christopoulos, M.M. Bemplidaki, Change ΔS of the entropy in natural time under time reversal: Complexity measures upon change of scale, Europhys. Lett. 109 (2015) 18002, http://dx.doi.org/10.1209/0295-5075/109/18002.

[23] P.A. Varotsos, N.V. Sarlis, E.S. Skordas, M.S. Lazaridou, Entropy in natural time domain, Phys. Rev. E 70 (2004) 011106, http://dx.doi.org/10.1103/physreve.70.011106.

[24] P.A. Varotsos, N.V. Sarlis, E.S. Skordas, M.S. Lazaridou, Natural entropy fluctuations discriminate similar-looking electric signals emitted from systems of different dynamics, Phys. Rev. E 71 (2005) 011110, http://dx.doi.org/10.1103/physreve.71.011110.

[25] C.-K. Peng, S.V. Buldyrev, A.L. Goldberger, S. Havlin, M. Simons, H.E. Stanley, Finite-size effects on long-range correlations: Implications for analyzing DNA sequences, Phys. Rev. E 47 (1993) 3730–3733, http://dx.doi.org/10.1103/physreve.47.3730.

[26] C.-K. Peng, S.V. Buldyrev, S. Havlin, M. Simons, H.E. Stanley, A.L. Goldberger, Mosaic organization of DNA nucleotides, Phys. Rev. E 49 (1994) 1685–1689, http://dx.doi.org/10.1103/physreve.49.1685.

[27] S.V. Buldyrev, A.L. Goldberger, S. Havlin, R.N. Mantegna, M.E. Matsa, C.-K. Peng, M. Simons, H.E. Stanley, Long-range correlation properties of coding and noncoding dna sequences: Genbank analysis, Phys. Rev. E 51 (1995) 5084–5091.

[28] M.S. Taqqu, V. Teverovsky, W. Willinger, Estimators for long-range dependence: An empirical study, Fractals 3 (1995) 785–798.

[29] P. Talkner, R.O. Weber, Power spectrum and detrended fluctuation analysis: Application to daily temperatures, Phys. Rev. E 62 (2000) 150–160, http://dx.doi.org/10.1103/physreve.62.150.
[30] K. Hu, P.C. Ivanov, Z. Chen, P. Carpena, H.E. Stanley, Effect of trends on detrended fluctuation analysis, Phys. Rev. E 64 (2001) 011114, http://dx.doi.org/10.1103/physreve.64.011114.
[31] Z. Chen, P.C. Ivanov, K. Hu, H.E. Stanley, Effect of nonstationarities on detrended fluctuation analysis, Phys. Rev. E 65 (2002) 041107.
[32] Z. Chen, K. Hu, P. Carpena, P. Bernaola-Galvan, H.E. Stanley, P.C. Ivanov, Effect of nonlinear filters on detrended fluctuation analysis, Phys. Rev. E 71 (2005) 011104.
[33] L. Xu, P.C. Ivanov, K. Hu, Z. Chen, A. Carbone, H.E. Stanley, Quantifying signals with power-law correlations: A comparative study of detrended fluctuation analysis and detrended moving average techniques, Phys. Rev. E 71 (2005) 051101, http://dx.doi.org/10.1103/physreve.71.051101.
[34] P. Carpena, P. Bernaola-Galván, P.C. Ivanov, H.E. Stanley, Metal–insulator transition in chains with correlated disorder, Nature 418 (2002) 955.
[35] K. Hu, P.C. Ivanov, Z. Chen, M.F. Hilton, H.E. Stanley, S.A. Shea, Non-random fluctuations and multi-scale dynamics regulation of human activity, Physica A 337 (2004) 307.
[36] Y. Ashkenazy, J.M. Hausdorff, P.C. Ivanov, H.E. Stanley, A stochastic model of human gait dynamics, Physica A 316 (2002) 662–670, http://dx.doi.org/10.1016/S0378-4371(02)01453-X.
[37] P.C. Ivanov, L.A. Nunes Amaral, A.L. Goldberger, H.E. Stanley, Stochastic feedback and the regulation of biological rhythms, Europhys. Lett. 43 (1998) 363.
[38] Y. Ashkenazy, P.C. Ivanov, S. Havlin, C.-K. Peng, A.L. Goldberger, H.E. Stanley, Magnitude and sign correlations in heartbeat fluctuations, Phys. Rev. Lett. 86 (2001) 1900–1903, http://dx.doi.org/10.1103/PhysRevLett.86.1900.
[39] Y. Ashkenazy, S. Havlin, P.C. Ivanov, C.-K. Peng, V. Schulte-Frohlinde, H. Stanley, Magnitude and sign scaling in power-law correlated time series, Physica A 323 (2003) 19–41, http://dx.doi.org/10.1016/S0378-4371(03)00008-6.
[40] K. Ivanova, M. Ausloos, Application of the detrended fluctuation analysis (DFA) method for describing cloud breaking, Physica A 274 (1999) 349–354, http://dx.doi.org/10.1016/s0378-4371(99)00312-x.
[41] E. Koscielny-Bunde, A. Bunde, S. Havlin, H.E. Roman, Y. Goldreich, H.J. Schellnhuber, Indication of a universal persistence law governing atmospheric variability, Phys. Rev. Lett. 81 (1998) 729.
[42] C.A. Varotsos, S. Lovejoy, N.V. Sarlis, C.G. Tzanis, M.N. Efstathiou, On the scaling of the solar incident flux, Atmos. Chem. Phys. 15 (13) (2015) 7301–7306, http://dx.doi.org/10.5194/acp-15-7301-2015.
[43] R.L. Stratonovich, Topics in the Theory of Random Noise I, Gordon and Breach, New York, 1981.
[44] P.A. Varotsos, N.V. Sarlis, E.S. Skordas, Long-range correlations in the electric signals that precede rupture, Phys. Rev. E 66 (2002) 011902, http://dx.doi.org/10.1103/physreve.66.011902.
[45] P.A. Varotsos, N.V. Sarlis, E.S. Skordas, Long-range correlations in the electric signals the precede rupture: Further investigations, Phys. Rev. E 67 (2003) 021109.
[46] P.A. Varotsos, N.V. Sarlis, E.S. Skordas, Attempt to distinguish electric signals of a dichotomous nature, Phys. Rev. E 68 (2003) 031106, http://dx.doi.org/10.1103/PhysRevE.68.031106.
[47] P. Varotsos, K. Alexopoulos, Physical properties of the variations of the electric field of the earth preceding earthquakes, I, Tectonophysics 110 (1984) 73–98, http://dx.doi.org/10.1016/0040-1951(84)90059-3.
[48] P. Varotsos, K. Alexopoulos, Physical properties of the variations of the electric field of the earth preceding earthquakes, II, Tectonophysics 110 (1984) 99–125.
[49] P.A. Varotsos, N.V. Sarlis, E.S. Skordas, M.S. Lazaridou, Fluctuations, under time reversal, of the natural time and the entropy distinguish similar looking electric signals of different dynamics, J. Appl. Phys. 103 (2008) 014906, http://dx.doi.org/10.1063/1.2827363.
[50] P. Varotsos, M. Lazaridou, Latest aspects of earthquake prediction in Greece based on Seismic electric signals, Tectonophysics 188 (1991) 321–347, http://dx.doi.org/10.1016/0040-1951(91)90462-2.
[51] P. Varotsos, K. Alexopoulos, M. Lazaridou, Latest aspects of earthquake prediction in Greece based on Seismic electric signals,II, Tectonophysics 224 (1993) 1–37, http://dx.doi.org/10.1016/0040-1951(93)90055-O.
[52] M. Lazaridou, C. Varotsos, K. Alexopoulos, P. Varotsos, Point-defect parameters of LiF, J. Phys. C: Solid State 18 (1985) 3891.
[53] P. Varotsos, Point defect parameters in β-PbF_2 revisited, Solid State Ion. 179 (2008) 438–441, http://dx.doi.org/10.1016/j.ssi.2008.02.055.
[54] N.V. Sarlis, E.S. Skordas, P.A. Varotsos, Order parameter fluctuations of seismicity in natural time before and after mainshocks, Europhys. Lett. 91 (2010) 59001, http://dx.doi.org/10.1209/0295-5075/91/59001.
[55] N.V. Sarlis, E.S. Skordas, P.A. Varotsos, Nonextensivity and natural time: The case of seismicity, Phys. Rev. E 82 (2010) 021110, http://dx.doi.org/10.1103/physreve.82.021110.
[56] C. Tsallis, Introduction to Nonextensive Statistical Mechanics, Springer, Berlin, 2009, http://dx.doi.org/10.1007/978-0-387-85359-8.
[57] C. Tsallis, Possible generalization of Boltzmann–Gibbs statistics, J. Statist. Phys 52 (1988) 479–487, http://dx.doi.org/10.1007/BF01016429.
[58] P.A. Varotsos, N.V. Sarlis, E.S. Skordas, Study of the temporal correlations in the magnitude time series before major earthquakes in Japan, J. Geophys. Res.: Space Phys. 119 (2014) 9192–9206, http://dx.doi.org/10.1002/2014JA020580.
[59] P.A. Varotsos, N.V. Sarlis, E.S. Skordas, M.S. Lazaridou, Seismic electric signals: An additional fact showing their physical interconnection with seismicity, Tectonophysics 589 (2013) 116–125, http://dx.doi.org/10.1016/j.tecto.2012.12.020.
[60] N.V. Sarlis, E.S. Skordas, P.A. Varotsos, T. Nagao, M. Kamogawa, H. Tanaka, S. Uyeda, Minimum of the order parameter fluctuations of seismicity before major earthquakes in Japan, Proc. Natl. Acad. Sci. USA 110 (2013) 13734–13738, http://dx.doi.org/10.1073/pnas.1312740110.
[61] N.V. Sarlis, E.S. Skordas, P.A. Varotsos, T. Nagao, M. Kamogawa, S. Uyeda, Spatiotemporal variations of seismicity before major earthquakes in the Japanese area and their relation with the epicentral locations, Proc. Natl. Acad. Sci. USA 112 (2015) 986–989, http://dx.doi.org/10.1073/pnas.1422893112.
[62] S. Tanaka, Tidal triggering of earthquakes prior to the 2011 Tohoku-Oki earthquake (Mw 9.1), Geophys. Res. Lett. 39 (2012) L00G26, http://dx.doi.org/10.1029/2012GL051179.